Fragment ion distribution in charge-changing collisions of 2-MeV Si ions with C_{60}

A. Itoh,[1,*] H. Tsuchida,[2] K. Miyabe,[1] T. Majima,[1] and Y. Nakai[3]
[1]*Quantum Science and Engineering Center, Kyoto University, Kyoto 606-8501, Japan*
[2]*Department of Physics, Nara Women's University, Nara 630-8506, Japan*
[3]*The Institute of Physical and Chemical Research, Saitama 351-0198, Japan*
(Received 6 March 2001; published 31 July 2001)

We have measured positive fragment ions produced in collisions of 2 MeV Si^{q+} ($q=0$, 1, 2, 4) projectiles with a C_{60} molecular target. The measurement was performed with a time-of-flight coincidence method between fragment ions and charge-selected outgoing projectiles. For all the charge-changing collisions investigated here, the mass distribution of small fragment ions C_n^+ ($n=1-12$) can be approximated fairly well by a power-law form of $n^{-\lambda}$ as a function of the cluster size n. The power λ derived from each mass distribution is found to change strongly according to different charge-changing collisions. As a remarkable experimental finding, the values of λ(loss) in electron loss collisions are almost the same for the same final charge states k irrespective of the initial charge q, exhibiting a nearly perfect linear relationship with k. We also performed calculations of the projectile ionization on the basis of the semiclassical approximation and obtained inelastic energy deposition for individual collision processes. The estimated energy deposition is found to have a simple correlation with the experimentally determined values of λ(loss).

DOI: 10.1103/PhysRevA.64.032702 PACS number(s): 34.70.+e, 61.48.+c

I. INTRODUCTION

Fragmentation of a free C_{60} molecule resulting from interactions with photons or energetic charged particles is a fundamental manifestation of inelastic collisions involving cluster particles. Since the C_{60} molecule with the spherical radius of ~ 6.6 a.u. may be regarded as an extremely thin film target, investigation of the collision-induced fragmentation process is important to understand the energy transfer mechanism relevant to intermediate matter lying between atoms and solids, for which the information is largely lacking [1]. It is now widely recognized [2–10] that C_{60} fragmentation may be characterized by two types of decay scheme: C_2 evaporation and multifragmentation. In the former scheme, intact ionized parent ions and their fullerenelike daughter ions C_{60-2m}^{r+} ($m \geqslant 0$) are produced dominantly, while in the latter scheme, small-size clusters C_n^+ ($n \geqslant 1$) are the main products arising from catastrophic disintegration of molecules. From a phenomenological viewpoint, it seems that the multifragmentation becomes dominant with increasing impact energy, incident charge and atomic number of collision partners [2–19]. This means that the decay scheme is essentially governed by the amount of internal energy of C_{60} deposited in collisions. A helpful example to understand this situation is the work of multiphoton laser absorption experiments [20–22], demonstrating clearly that the decay scheme changes from evaporation to multifragmentation with increasing laser intensity. Theoretically, the maximum entropy calculations made by Campbell *et al.* [23] indicate that the onset of multifragmentation occurs at an internal energy of about 85 eV and pure multifragmentation occurs beyond 200 eV. There is a transition region between these two energies where both mechanisms coexist.

In collisions with energetic ions, a large enough energy deposition leading to C_{60} multifragmentation is likely possible only in close cage-penetrating collisions of both slow [3–8] and fast projectile ions [9,14–19]. In such collisions, particularly of fast heavy ions, the intensity distribution of C_n^+ exhibits usually a power-law form of $n^{-\lambda}$ as a function of the cluster size n [9,14–17]. This power-law distribution was systematically investigated by us [17] for various projectiles ions (H–Au) and was successively interpreted from the projectile energy loss concept. To date, however, direct measurements of the projectile energy loss in collisions with C_{60} are sparse and limited to slow velocity ions [6,7,24,25]. Among them, Martin *et al.* [6] measured the energy loss in electron capture collisions of Ar^{8+} ions ($v=0.24$ a.u.), and showed that the lightest fragment ions such as C^+ and C_2^+ are preferentially produced in cage-penetrating collisions accompanying a considerably large energy loss of about 300 eV. On the other hand, Larsson *et al.* [25] reported that the projectile energy loss in two-electron capture collisions of 100 keV Ar^{3+} is larger than that in single-capture collisions. They attributed this difference to the shrinking of the capture radius with increasing number of captured electrons, meaning closer collisions of the double-capture process. These energy loss experiments suggests directly that the distance between collision partners is the key parameter which determines the amount of energy deposition E. Consequently, the intensity distribution of small fragment ions C_n^+ would be different for different collision processes, since E may also be different for individual collisions. Indeed, we found the degree of C_{60} multifragmentation to change drastically for individual charge-changing processes of fast Li projectiles [18,19].

In the present work, we extended measurements to Si^{q+} projectile ions, for which the power-law behavior is expected to appear more clearly [17]. The values of the power λ were obtained for 14 different electron loss and capture collisions. Since the electron loss is the projectile ionization by a target

*Electronic address: itoh@nucleng.kyoto-u.ac.jp

particle, we performed calculations of the impact-parameter-dependent electron loss probabilities using a table available in the literature [26]. With these probabilities and an available energy loss function [27,28], we estimated the amount of electronic energy deposition for individual loss collisions. It will be shown that the experimentally determined power λ is strongly correlated with the calculated energy deposition, indicating a possible approach to derive information about the energy transfer mechanism in fast-ion–C_{60} collisions.

II. EXPERIMENT

The apparatus and the experimental method are the same as described in detail elsewhere [18,19], and only a brief outline is given here. A beam of 2 MeV Si^{q+} ($q=1$, 2 and 4) ions with velocity $v=1.69$ a.u. was extracted from an 1.7-MV tandem Cockcroft-Walton accelerator of Kyoto University. The beam was charge purified in a charge-selection chamber, consisting of four electrostatic deflectors, by removing impurity ions of undesirable charge states formed in the beam line. A neutral atomic beam of Si^0 was also used as a projectile. In this case the neutral particles were selected out of a Si^+ primary beam with a conventional permanent magnet. The charge-purified beam was then incident on a gas phase C_{60} target in a crossed beam collision chamber. The C_{60} target was produced by heating 99.9%-pure C_{60} powder at 465 °C in a temperature controlled quartz oven located at the base of the collision chamber. Through a hole (2 mm in diameter) opened at the top of the oven, the C_{60} molecular beam was introduced upward into a collision region. After collisions with the C_{60} target, outgoing projectiles were charge separated by a magnet and detected by a movable solid-state detector (SSD). Mass-to-charge analysis of fragment ions was made with a Wiley-McLaren type time-of-flight (TOF) spectrometer in conjunction with a two-stage multichannel plate detector. The extraction field used for the fragment ions was 375 V/cm. The base pressure in the beamline and the collision chamber was below 3×10^{-7} Torr during the experiment.

TOF spectra of the fragment ions were measured in coincidence with outgoing charge states of silicon projectiles. Combinations between initial and final charge states $(q;k)$ investigated in the present work are (0; 1–3), (1; 2–5), (2; 0,1,3,4), and (4; 2,3,5). For other combinations, particularly for non-charge-changing collisions ($k=q$), it was often difficult to obtain reliable data with good counting statistics. Data acquisition was made with a fast multichannel scaler (FMCS, LN-6500, Labo.) with highest time resolution of 1 ns, enabling us to detect plural fragment ions produced in a single-collision event. In the present experiment the FMCS was operated with a time resolution of 8 ns/channel. The experimental error, arising mainly from counting statistics, was about 10%–20%.

III. RESULTS AND DISCUSSION

A. Mass distribution of fragment ions

We have measured 14 different TOF spectra of fragment ions for various combinations of initial and final charge states of 2 MeV Si^{q+} projectiles. Some examples of TOF spectra are shown in Fig. 1, where the peak height of the most intensive peak in each spectrum is normalized to 100. Note that, in the spectra for $2\rightarrow0$ and $4\rightarrow3$, undesirable lines arising from residual gases of H_2O, N_2, and O_2 are not shown to avoid confusion. The mass-to-charge distribution of fragment ions is composed of two parts corresponding to the fragmentation part (C_n^+, $n=1$–12) and the ionization part (C_{60-2m}^{r+}, $m\geq0$, $r=1$–4) including fullerenelike daughter ions produced via C_2 evaporation [4–9]. The relative intensity between these two parts was found to change significantly for different charge-changing collisions. Namely, the fragmentation part was always observed in all the $q\rightarrow k$ processes, while the ionization part was observed only for some limited cases. Another characteristic extracted from the TOF spectra is that the relative intensity among intact parent ions C_{60}^{r+} differs also for different $q\rightarrow k$ capture collisions. That is, in two-electron capture collisions, enhancement of highly ionized parent ions ($r=3$ and 4) is observed strongly in comparison with one-capture collisions. It is noted that the singly charged C_{60}^+ ion was completely

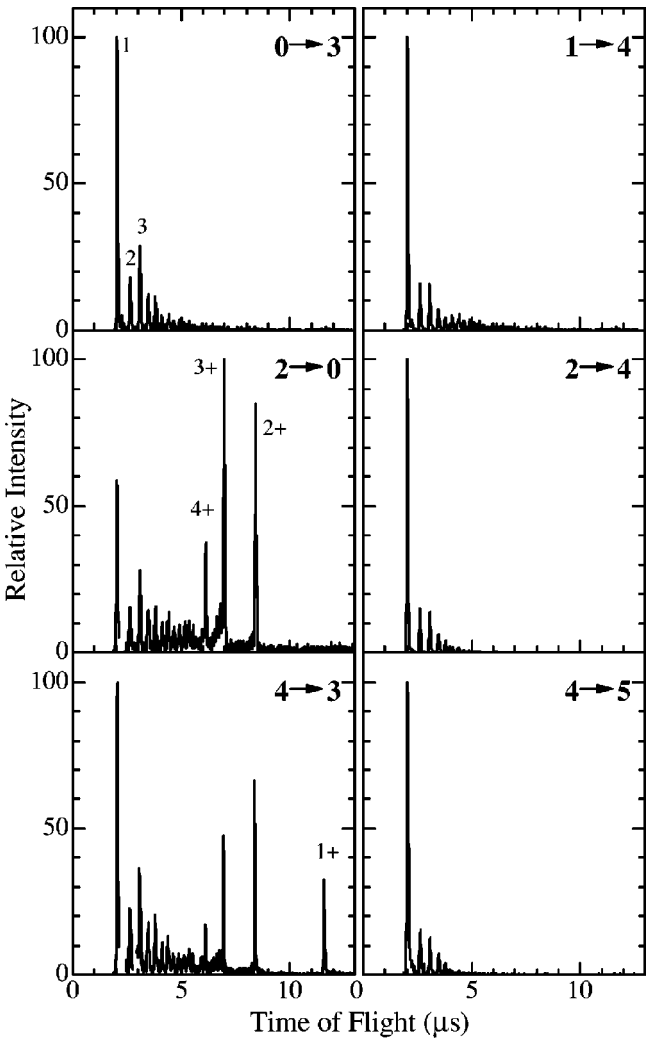

FIG. 1. Time-of-flight mass spectra obtained in $q\rightarrow k$ charge-changing collisions of 2 MeV Si^{q+} with a C_{60} target.

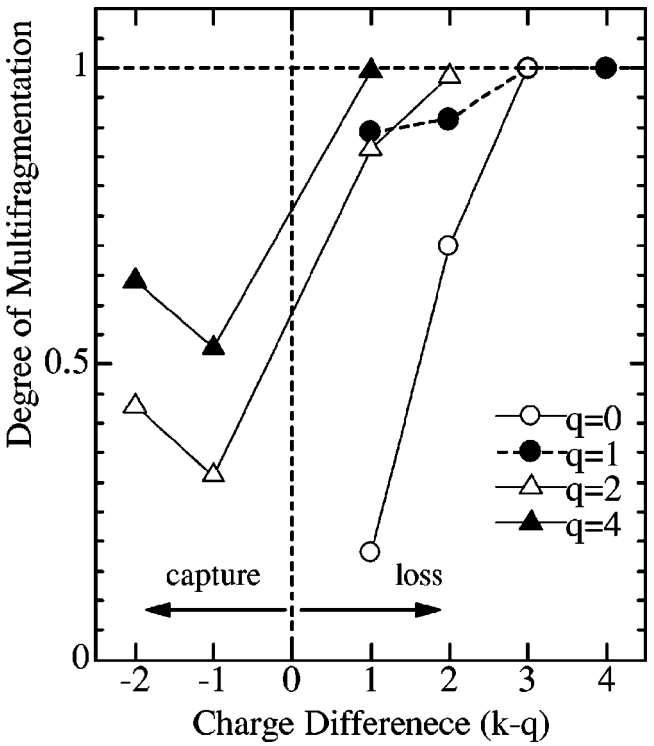

FIG. 2. Degree of multifragmentation (see text) as a function of the charge difference $k-q$ before and after collisions.

absent in two-electron capture collisions ($2\rightarrow0$ and $4\rightarrow2$). This ensures single-collision conditions of our experiment and, moreover, indicates that the slow C_{60}^{2+} ions extracted from the collision region do not undergo electron capture collisions during flight in the TOF spectrometer.

We define here the ''degree of multifragmentation'' as the ratio between the total intensity Y_t of all C_n^+ ions ($n=12$) observed in the fragmentation part and that of all ions in the whole spectrum. Results are depicted in Fig. 2 as a function of charge difference ($k-q$), showing that the multifragmentation is predominant particularly in electron loss collisions. It is also indicated that the multifragmentation becomes more significant with increasing charge difference $|k-q|$ both in loss and capture collisions. This feature is, on the other hand, typically observed in capture collisions of highly charged slow ions [3,8]. As a surprising result, it should be noted that the degree of multifragmentation is nearly 100% even for the one-electron loss collision $4\rightarrow5$, as can be also seen in Fig. 1. All these results imply evidently that the electron loss is a much more violent collision compared to the capture process. Such a violent collision is supposed to occur at small impact parameters with accompanying a large amount of energy deposition into a C_{60} molecule as is discussed below.

Peak intensities of small fragment ions C_n^+ ($n=1-12$) are plotted in relative scale in Fig. 3. Except for even-odd oscillations, the intensity decreases rather monotonically as a function of n, as observed similarly in other fast heavy-ion collisions [9,14,16,17]. Obviously, the rate of intensity decrease is considerably larger in electron loss collisions (open symbols) than in capture collisions (solid symbols), implying again that the electron loss collisions are more violent than

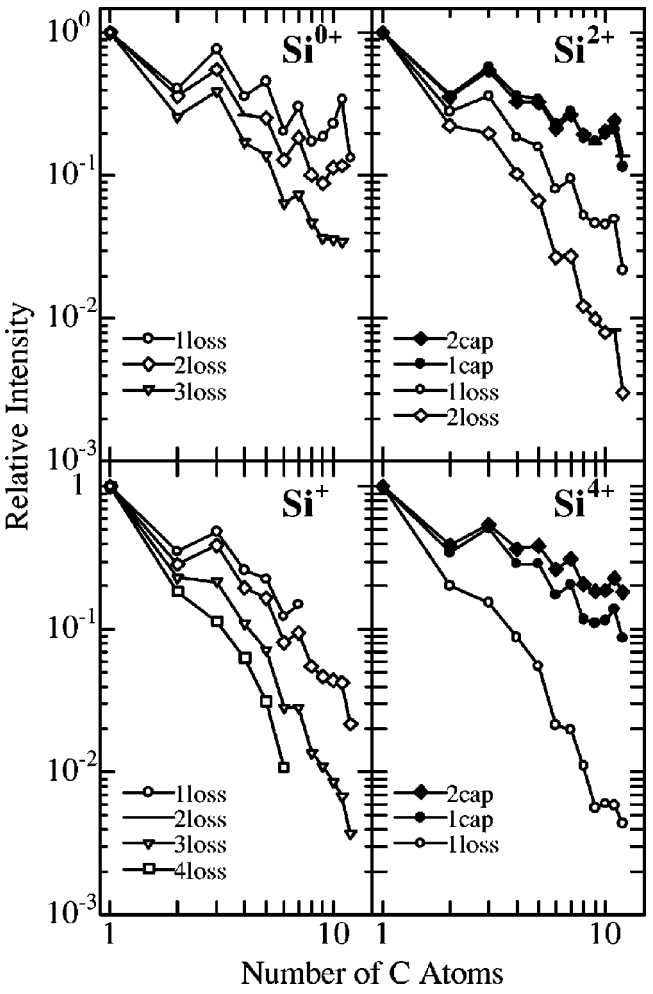

FIG. 3. Relative intensity of C_n^+ fragment ions as a function of the cluster size n. The intensities of C^+ are taken to be unity.

the capture processes. Assuming a power-law form of $n^{-\lambda}$ for the intensity distribution, we obtained the values of λ for all the present $q\rightarrow k$ collisions. The results are shown in Fig. 4, where the abscissa is the peak intensity Y_1 of C^+ divided by the total intensity Y_t in the fragmentation part. The dashed curve represents theoretical values of Y_1 $(=1)$ divided by $(1+2^{-\lambda}+3^{-\lambda}+\cdots)^{-1}$. It can be seen obviously that the theoretical curve reproduces all the experimental data almost perfectly, implying good accuracy of the power-law approximation to express the present C_n^+ intensity distribution.

Figure 5 shows λ as a function of the projectile incident charge q. One can see clearly that the q dependence is completely different for loss and capture collisions. In loss collisions the power λ increases rapidly with increasing q and becomes larger as the number of lost electrons increases. On the contrary, no such trends are observed in capture collisions, and values of λ are small and remain nearly constant irrespective of different q. For loss collisions, one can notice (see also Fig. 4) that the values of λ are nearly the same when the final charge states are the same. This surprising characteristic is clearly demonstrated in Fig. 6 by plotting λ as a function of k. At $k=5$, for instance, nearly the same value of about 2 is obtained for one-electron loss collisions

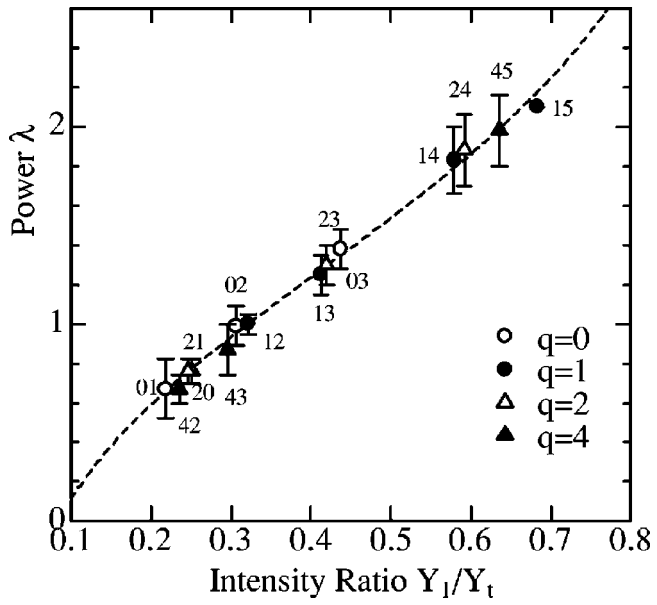

FIG. 4. The power λ as a function of the intensity ratio Y_1/Y_t between C^+ and total sum of $C_n^+(n=1-12)$. Theoretical values are drawn by a dashed line.

$(4\rightarrow5)$ and four-electron loss collisions $(1\rightarrow5)$. Similarly, at $k=3$ a constant value of about 1.3 is obtained for three incident charges $(q=0,1,2)$. This result implies that the final charge plays the key role in determining the final mass distribution of fragment ions in electron loss collisions. It indicates convincingly that a target C_{60} may receive an equivalent amount of energy deposition E irrespective of the number of lost electrons when the projectile final charge is the same. In other words, the loss collisions of the same k seem to take place at equivalent impact parameters. More detailed analysis is given in the following section.

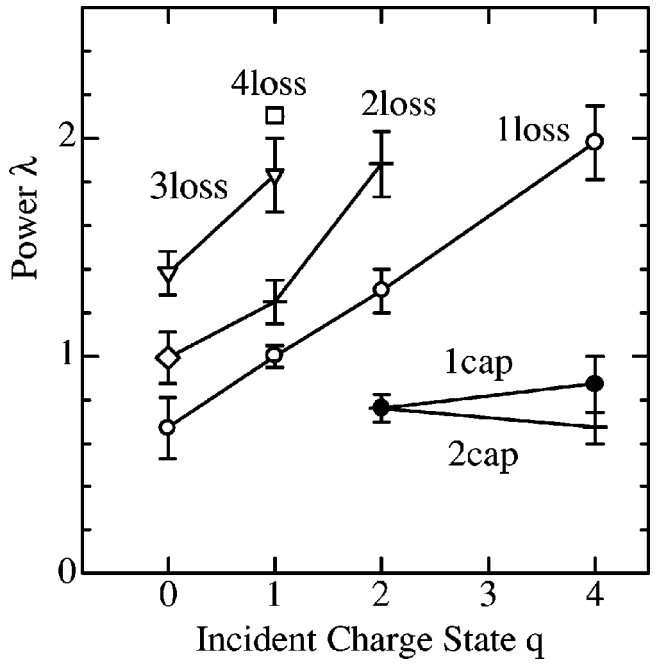

FIG. 5. The power λ as a function of the incident charge q.

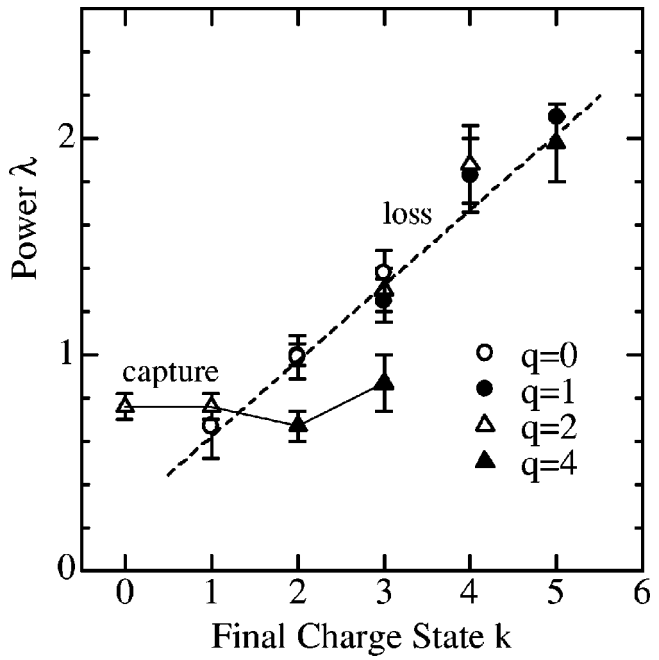

FIG. 6. The power λ as a function of the final charge k. Two lines are drawn to guide the eye. Note a linear relationship for loss collisions.

One more striking characteristic derived from Fig. 6 is a linear relationship between λ(loss) and k as shown by a dotted straight line to guide the eye. All the experimental values of λ for loss collisions lie excellently well on this line within their experimental errors. On the other hand, there seems to be no such trend for capture collisions, although a slight increase is seen for the incident beam of $q=4$.

B. Inelastic energy deposition

It is stressed again that the mass distribution of C_n^+ ions carries certainly information about the inelastic energy deposition into a C_{60} molecule. Hence, various characteristics of λ described above may apply also for the amount of energy deposition. A particularly indicative experimental finding is that the λ's or the amount of energy deposition in other words, are different from one another in different charge-changing collisions. Therefore, it might be possible to deduce the energy deposition E for individual collision processes. Since no rigorous calculation of this kind has ever been done before, we attempted calculations of E in the following two ways.

As the simplest method of estimation [17,19,29], we used the TRIM code [30] to obtain an electronic stopping cross section S_1 $(=1.76\times10^{-13}$ [eVcm^2]) for a collision system of 2 MeV Si+C. The corresponding value for nuclear stopping is only 4.85×10^{-15} [eVcm^2] and is ignored in the following discussion. The energy deposition E_{qk}^{trim} per C_{60} molecule for $q\rightarrow k$ collision may be obtained by $E_{qk}^{TRIM}=Z_{qk}^2S_1\times60/\pi a^2=Z_{qk}^2\times2744$ [eV], with the molecular radius $a=6.6$ a.u. Here, the effect of different charge states in individual collisions is taken into consideration as the square of Z_{qk}, the mean charge in the $q\rightarrow k$ collision. The mean

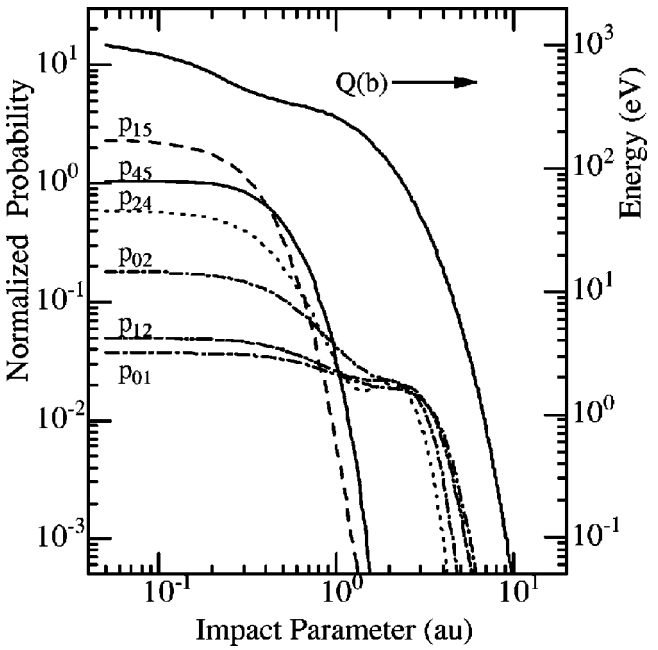

FIG. 7. Normalized probability function p_{qk} for loss collisions as a function of the impact parameter (atomic units). $Q(b)$ is the electronic stopping function [26,27].

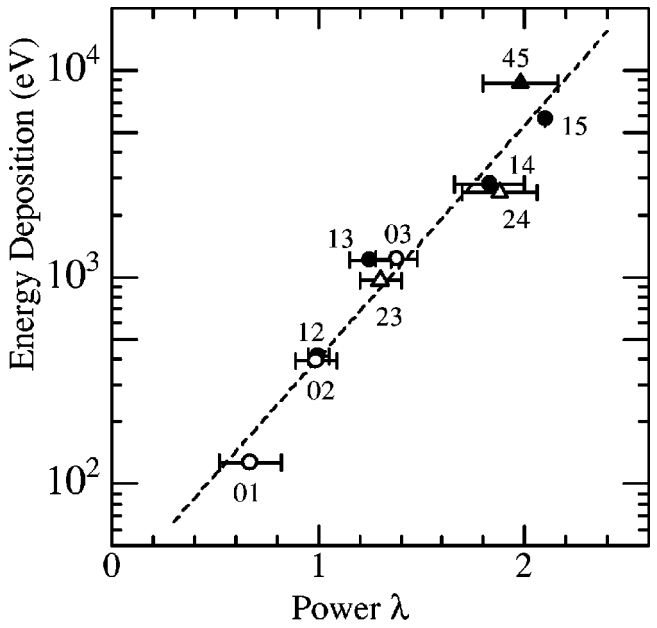

FIG. 8. Calculated energy deposition E_{qk} for $q \rightarrow k$ loss collisions as a function of the experimentally determined power λ. The dashed line is the fitting result; $E(\lambda) = 30 \exp(2.6\lambda)$.

charge Z_{qk} was simply taken as an average value between the initial and final effective charges obtained, respectively, by the hydrogenic formula $n_i\sqrt{2I(i)}$ for the charge state $i = q-1$ and $k-1$, where n_i and $I(i)$ are the principal quantum number and the ionization potential (a.u.) of Si^{i+} [33]. In actual calculations, we employed the relative mean values with respect to 3.51 which is the mean charge of Si used in the TRIM code determined by $\sqrt{S_1(\mathrm{Si})/S_1(\mathrm{H})}$ at the present velocity of 1.69 a.u. [30]. For instance, Z_{45} is calculated to $(5.47+7.0)/3.51/2 = 1.78$, giving rise to an energy deposition of $E_{45}^{TRIM} = 8658$ eV.

In this calculation, however, the charge-changing collision is characterized only by the initial and final charge states, and consequently, there is no distinction between electron loss and capture collisions if the (q,k) combination is the same, e.g., $E_{24}^{TRIM} = E_{42}^{TRIM}$. However, the experimental results of λ show clear differences between loss and capture collisions, indicating that the effective collision distance or the impact parameter between collision partners within which the $q \rightarrow k$ collision occurs most likely should be taken into consideration. This is achieved in our second method of calculations described in the following.

The stopping cross section $S_1(qk)$ for a $q \rightarrow k$ collision can be expressed by the following formula if the impact-parameter-dependent stopping function $Q_{qk}(b)$ is known for the $q \rightarrow k$ collision:

$$S_1(qk) = 2\pi \int_0^\infty b Q_{qk}(b) db. \tag{1}$$

To our best knowledge, however, there is no previous work referring to such specific $Q_{qk}(b)$. Schiwietz and co-workers have formulated the impact-parameter-dependent stopping function $Q(b)$ for fast heavy projectiles [27,28]. We used their program code CASP for the collision system of 2 MeV Si+C. The total electronic stopping cross section calculated by Eq. (1) with this $Q(b)$ was normalized to the TRIM value of S_1 given above. Using $Q(b)$ and the probability $p_{qk}(b)$ for the $q \rightarrow k$ charge-changing collision at b, the desired stopping function $Q_{qk}(b)$ may be approximated by $p_{qk}(b)Q(b)$. However, this formula implies that the corresponding energy deposition E_{qk} as well as $S_1(qk)$ would become a small value if the probability p_{qk} is small, leading to an unrealistic conclusion. For instance, E_{15} in a four-electron loss collision would become a negligibly small value compared to E_{12} in a one-electron loss collision, since the corresponding probabilities are supposed to be largely different. Actually, this difference was found, in our following calculations, to be more than two orders of magnitude. Such a conclusion contradicts what is expected from our mass distribution as described in Sec. III A. Hence, for all the $q \rightarrow k$ collisions the probability function $p_{qk}(b)$ must be normalized to an appropriate constant value in such a way like

$$2\pi \int_0^\infty b p_{qk}(b) db = C \quad \text{a.u.}. \tag{2}$$

Integration of the real probability gives, of course, a $q \rightarrow k$ charge-changing cross section which in turn connects directly with the experimental yield of fragment ions.

In this way, the energy deposition in the $q \rightarrow k$ charge-changing collision of both electron capture and loss can be evaluated by the formula

$$S_1(qk) = 2\pi \int_0^\infty b p_{qk}(b) Q(b) db \tag{3}$$

provided that the probability function $p_{qk}(b)$ is known. Compared to electron capture collisions, the electron loss process is essentially simple, because it is the projectile ionization by a target particle in the projectile rest frame. Since rigorous theoretical calculations on capture and loss collisions are out of the scope of the present work, we treat only the electron loss processes in the following.

Hansteen *et al.* tabulated impact-parameter-dependent ionization probabilities for *K*-, *L*-, and *M*-shell electrons by fast bare projectile ions [26]. Following these well-known semiclassical approximation (SCA) calculations, we first obtained ionization probabilities of *s* and *p* electrons in both *M* and *L* shells of a Si^{q+} ion. The calculation was made for a projectile ion with charge $z_p=1$ at velocity of 1.69 a.u. This is due to the fact that the probability is scaled only by z_p^2 [26], and consequently, the value of z_p plays no role according to Eq. (2). Next, we deduced the average single-ionization probabilities for the *M* shell (p_m) and *L* shell (p_l), respectively, by taking account of the number of *s* and *p* electrons in each shell. The binding energies of the *nl* shells of Si^{q+} are taken from [31]. Finally, the multiple-ionization probability $p_{qk}(b)$ for Si^{q+} is calculated using the independent electron model [32] as

$$p_{qk}(b)=\sum_{i=0}\begin{bmatrix}M\\ i\end{bmatrix}\begin{bmatrix}L\\ j\end{bmatrix}p_m^i(1-p_m)^{M-i}p_l^j(1-p_l)^{L-j},$$

$$i+j=k-q. \quad (4)$$

Here, $\begin{bmatrix}N\\ r\end{bmatrix}$ is the binomial coefficient, and *M* and *L* are the number of electrons in *M* and *L* shells, respectively—e.g., $M=1$ and $L=8$ for Si^{3+}.

Some examples of the calculated results are shown in Fig. 7 together with the stopping function $Q(b)$ [27,28]. Note that all these p_{qk} functions are the normalized functions according to Eq (2); in this figure we took $C=1$. One can immediately notice the relative importance between *M*- and *L*-shell contributions in various $q\rightarrow k$ ionizations. As the simplest cases, the single ionization p_{01} of a neutral Si atom is found to take place in a wide range of *b* and is dominated by *M*-shell ionization, while the single *L*-shell ionization p_{45} of Si^{4+} is restricted to a small *b* range below 1 a.u. It should be pointed out that the four-electron ionization p_{15} of Si^{+} reveals a similar form as the single ionization of Si^{4+} and is also restricted to $b<1$ a.u., indicating that a large amount of inelastic energy may be deposited as expected from our experimental results of λ.

Finally, the energy deposition E_{qk} per C_{60} molecule is obtained by the same formula as the first method, $E_{qk}=Z_{qk}^2S_1(qk)\times 60/\pi a^2$. As for the normalization factor *C*, which is an arbitrary value in our calculations, we simply normalized the value of $E_{45}(C=1)$ to E_{45}^{TRIM}, giving rise to $C\simeq 10$. It is interesting to note that this value of *C* gives an effective collision radius of $r=1.8$ a.u. from a relation $C=\pi r^2$, which is nearly the same order of the radius of a carbon atom [34]. Calculated results of E_{qk} are shown in Fig. 8 as a function of $\lambda(qk)$ measured experimentally. It appears that the energy deposition E_{qk} spreads from 100 eV to 9 keV

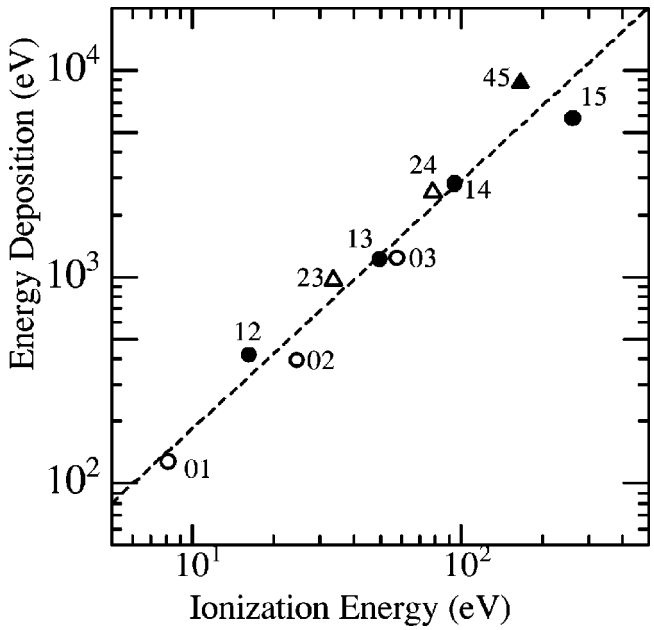

FIG. 9. Energy deposition E_{qk} as a function of the minimum ionization energy I_{qk} required to produce $q\rightarrow k$ charge state. The dashed line is the fitting result; $E=11.6I^{1.2}$.

according to various electron loss collisions. Above all, one can see a remarkably simple relationship between E_{qk} and $\lambda(qk)$, for which we obtained $E\ [\mathrm{eV}]=30\exp(2.6\lambda)$, shown by the dashed line in the figure. This astonishing finding may be regarded as sheer evidence of our basic idea of the possibility of deducing the energy deposition from the C_n^+ mass distribution pattern. Note, however, that the absolute values are uncertain due to an unknown factor *C* appearing in our calculations.

As the electron loss is the projectile ionization, the energy deposition calculated above is supposed to have some simple relationship with the ionization potential of projectile ions. This is demonstrated in Fig. 9, where the values of E_{qk} are plotted as a function of the minimum ionization energy I_{qk} in $q\rightarrow k$ capture collisions. The quantity I_{qk} is the minimum energy necessary to produce the charge state *k* from the initial charge *q*, given by the sum of ionization potentials, i.e., $I_{01}=I(0)$, $I_{14}=I(1)+I(2)+I(3)$, and so on. Obviously, the data of E_{qk} can be well reproduced by a straight line of the relationship $E_{qk}=11.6I_{qk}^{1.2}$, implying that the power $\lambda(qk)$ for loss collisions can also be related to I_{qk} as $I\ [\mathrm{eV}]=2.2\exp(2.17\lambda)$, using the formula derived for E_{qk}.

The fact of this simple correlation between E_{qk} and I_{qk} may be a certain justification of the present estimation method of the energy deposition in loss collisions. Thus, it is plausible to estimate E_{qk} for capture collisions, too, using the above formula and experimental $\lambda(\mathrm{cap})$ values. The evaluated value of E_{qk} is in turn expected to provide information about the capture radius b_c for the $q\rightarrow k$ collision if a step function form is assumed for the probability function $p_{qk}(b)$. Here, the electron capture probability is assumed to be constant at $b\leqslant b_c$ and zero outside. The capture radii $b_c(qk)$ (in atomic units) obtained in this way are 3.8 $(2\rightarrow 0)$, 5.2$(2\rightarrow 1)$, 9.2$(4\rightarrow 2)$, and 8.3$(4\rightarrow 3)$, respectively. Although

these values might contain uncertainties arising from a step function assumption, it shows clearly a general trend that the highly charged Si^{4+} ions can capture electrons at larger b than the Si^{2+} ions. It also shows that the capture by Si^{2+} takes place inside a C_{60} molecule, while it does outside for Si^{4+} ions. This outside capture by highly charged ions is, in turn, very typical in slow HCI experiments [3,6–8,15]. Also, it is pointed out that the radius for double-electron capture by Si^{2+} is smaller than that of single-electron capture, $b_c(20) < b_c(21)$. This result is consistent with the previous work done by Lersen *et al.* for 100 keV Ar^{3+} [12]. On the contrary, the relationship is just the opposite $[b_c(42) > b_c(43)]$ for Si^{4+} ions, implying a more distant collision for double electron capture events. Correspondingly, the calculated energy deposition is 171 and 288 eV for $4 \rightarrow 2$ and $4 \rightarrow 3$, respectively. It seems to mean that the double capture by Si^{4+} is more favorable at the present projectile velocity compared to the single-capture event.

It is also found that electron capture by $Si^{2+,4+}$ ions occurs in far more distant collisions than most loss collisions (see Fig. 7) and accompanies smaller amounts of energy deposition. For instance, we obtained surprisingly different energy depositions for $4 \rightarrow 3$(288 eV) and $4 \rightarrow 5$(8.66 keV) collisions, despite a similar magnitude of mean charges Z_{4k} in both processes. This can be attributed mainly to the largely different effective collision distances of these two collisions; i.e., the effective distance for $4 \rightarrow 5$ is smaller than 1 a.u. as shown in Fig. 7, while it is 8.3 a.u. for $4 \rightarrow 3$. This feature has, however, been already indicated in the λ values depicted in Figs. 4–6. Thus, we conclude that the power λ carries certain information about inelastic energy deposition and this information is successfully derived from the impact-parameter analysis method.

Finally, we discuss briefly the internal excitation and the multiple ionization of C_{60} using the electronic energy deposition E_{qk} described above. Since the energy deposition is spent for target excitation and ionization, it may be possible to estimate the internal excitation energy (ε_e) and the ionization energy (ε_I) provided that the corresponding partition rates are known. Unfortunately, there are no such data available for the C_{60} molecule and, consequently, only rough estimations are possible at the present stage. As outlined in our previous paper [17], the partition rates may be estimated to be 0.2 (excitation) and 0.8 (ionization), which are the theoretical values obtained for a $H+H_2O$ collision system at a hydrogen velocity of 1.69 a.u. [35]. If we employ these partition rates, the corresponding inelastic energies can be calculated for individual charge-changing collisions. For instance, the energy deposition of $E_{qk}=1 \sim 9$ keV gives $\varepsilon_e = 200$–1800 eV and $\varepsilon_I = 800$–7200 eV. Obviously, the internal excitation energy is large enough to induce complete disintegration of C_{60} via vibrational excitation as expected from theoretical predictions [23]. Actually, the mass distributions in such large E_{qk} collisions are dominated by only smaller fragment ions as can be seen in Fig. 1. Furthermore, the internal energy per carbon atom is estimated to be in the range from a few eV to 30 eV, obtained simply by $\varepsilon_e/60$. Consequently, it is expected that the kinetic energy of fragment ions, e.g., C^+, is of the order of several eV by taking account of the cohesive energy [36] and the ionization potential of the C atom. It is noted that the kinetic energy estimated in this way is in fairly good agreement with experimental values measured for 2-MeV Si^{4+} ions [37]. As for the ionization energy, ejected electrons are supposed to carry away about 75% of ε_I as their kinetic energies [38]. Hence, the degree of multiple ionization may be determined from the rest of the energy by solving the equation $\varepsilon_I \times 0.25 = I_1 + I_2 + \cdots + I_m$, with the ith ionization potential of C_{60}, $I_i = 3.77 + 3.82i$ [39]. If the linear relationship between I_i and i is assumed also for high i values, the degree of ionization is estimated to be $m=9+$ to $29+$ for $\varepsilon_I = 0.8$–7.2 keV. Namely, it implies that about half of the 60 carbon atoms in a C_{60} molecule may be ionized in large E_{qk} collisions such as one-electron loss collision of 2 MeV Si^{4+} ions. Such highly ionized parent ions may also decay immediately into small fragment ions via Coulomb explosion as typically observed in slow HCI collisions [40]. Note that the experimentally observed highest charge state of parent ions is $9+$ [41].

On the contrary, for collisions accompanying smaller energy deposition ($E_{qk} < 1$ keV), simple estimations given above may fail gradually with decreasing E_{qk}, because both ε_e and the multiple ionization become small. In fact, for $0 \rightarrow 1$ collisions ($E_{01} = 126$ eV), the internal energy is only 25 eV and the maximum degree of ionization is 2–$3+$. These values seem to be too low to induce multifragmentation, which is, however, observed experimentally. Apparently, it seems to imply that either the partition rate (0.2) or the total energy deposition E_{qk} itself is too small. As for the latter case, we suppose that molecular or neighboring effects may play an important role in collisions with C_{60}. If an incident ion interacts with more than one carbon atom, the total electronic deposition may become larger than the present estimated values which are obtained by assuming a simple additive rule ($60/\pi a^2$), ignoring any molecular effects.

In conclusion, more systematic experimental and theoretical data will be needed to obtain more reliable energies of ε_e and ε_I. In particular, measurements of the number of emitted electrons as well as the electron energy distribution are important to determine directly the degree of multiple ionization in fast ion collisions.

IV. SUMMARY

We have studied the C_{60} multifragmentation process induced by charge-changing collisions of 2-MeV Si^{0-4+} ions. It is found that the multifragmentation is the predominant decay process in multiple electron loss collisions. Surprisingly, this is also the case even for the one-electron loss collisions of Si^{4+}, indicating clearly that such a projectile ionization is induced only in very small impact-parameter collisions with probably a single carbon atom in C_{60}.

The mass distribution of small-size C_n^+ ions is found to be well approximated by a power-law form of $n^{-\lambda}$ as observed commonly in previous similar experiments [9,14–17]. We obtained the values of power λ for individual charge changing collisions and examined them in detail. In particu-

lar, $\lambda(\mathrm{loss})$ is found to have some remarkable dependences on the projectile final charge k. First, the values of the $\lambda(\mathrm{loss})$ are nearly the same for the same k, $\lambda(qk) \simeq \lambda(q'k)$, independently of the initial charge. Second, there is an excellent linear relationship between $\lambda(\mathrm{loss})$ and k as shown in Fig. 6.

Projectile ionization probabilities have been calculated with the aid of the available table of SCA calculations [26]. Combining these probabilities with the electronic stopping cross sections calculated with the program codes TRIM [30] and CASP [27,28], we deduced the amount of energy deposition E_{qk} for individual electron loss collisions. Although the absolute values might be uncertain due to an arbitrary normalization factor used in our calculations, the estimated values are found to show a surprisingly simple relationship with the experimentally determined $\lambda(\mathrm{loss})$ values. It is also found that the $\lambda(\mathrm{loss})$ is strongly correlated with the minimum ionization energy required to produce $q \rightarrow k$ charge states. These findings lead us to discuss electron capture collisions, and some important characteristics such as initial-charge dependency and the capture radius are reasonably derived.

Furthermore, a brief discussion is given for the internal excitation energy and the degree of multiple ionization using the electronic energy deposition. The multifragmentation observed in violent collisions accompanying large E_{qk} is successfully accounted for with these estimated quantities. On the other hand, it appears that the estimated E_{qk} seems to be too small for low-E_{qk} collisions. It is concluded that systematic research is desirable to determine important physical quantities such as the partition rates of the total energy deposition and molecular effects in collisions.

ACKNOWLEDGMENTS

One of the authors (A.I.) appreciates valuable discussions with Dr. G. Schiwietz at Hahn-Meitner-Institut Berlin, Dr. K. Okuno at Tokyo Metropolitan University, Dr. H.O. Lutz, and N. Kabachnik at Bielefeld University. We also would like to thank K. Yoshida at QSEC for his excellent operation of the accelerator.

[1] M.J. Berger and H. Paul, *Atomic and Molecular Data for Radiotherapy and Radiation Research* (International Atomic Energy Agency, Vienna, Austria, 1995), p. 415.

[2] P. Hvelplund, L.H. Andersen, H.K. Haugen, J. Lindhard, D.C. Lorents, R. Malhotra, and R. Ruoff, Phys. Rev. Lett. **69**, 1915 (1992).

[3] B. Walch, C.L. Cocke, R. Voelpel, and E. Salzborn, Phys. Rev. Lett. **72**, 1439 (1994).

[4] T. Bergen, X. Biquard, A. Breac, F. Chandezon, C. Guet, and B.A. Huber, in *Photonic, Electronic and Atomic Collisions*, edited by F. Aumayr and H. Winter (World Scientific, Singapore, 1998), p. 657.

[5] T. Schlathölter, O. Hadjar, J. Manske, R. Hoekstra, and R. Morgenstern, Int. J. Mass Spectrom. Ion Processes **192**, 245 (1999).

[6] S. Martin, J. Bernard, L. Chen, A. Denis, and J. Désesquelles, Eur. Phys. J. D **4**, 1 (1998).

[7] H. Cederquist, A. Fardi, K. Haghighat, A. Langereis, H.T. Schmidt, S.H. Schwartz, J.C. Levin, I.A. Sellin, H. Lebius, B. Huber, M.O. Larsson, and P. Hvelplund, Phys. Rev. A **61**, 22 712 (2000).

[8] S. Martin, L. Chen, A. Denis, R. Bredy, J. Bernard, and J. Désesquelles, Phys. Rev. A **62**, 22 707 (2000).

[9] S. Cheng, H.G. Berry, R.W. Dunford, H. Esbensen, D.S. Gemmell, E.P. Kanter, T. LeBrun, and W. Bauer, Phys. Rev. A **54**, 3182 (1996).

[10] H. Shen, P. Hvelplund, D. Mathur, A. Bárány, H. Cederquist, N. Selberg, and D.C. Lorents, Phys. Rev. A **52**, 3847 (1995).

[11] R. Ehlich, M. Westerburf, and E.E.B. Campbell, J. Chem. Phys. **104**, 1900 (1996).

[12] M.C. Lersen, P. Hvelplund, M.O. Larsson, and H. Shen, Eur. Phys. J. D **5**, 283 (1999).

[13] H. Tshuchida, A. Itoh, Y. Nakai, K. Miyabe, and N. Imanishi, J. Phys. B **31**, 5383 (1998).

[14] Y. Nakai, A. Itoh, T. Kambara, Y. Bitoh, and Y. Awaya, J. Phys. B **30**, 3049 (1997).

[15] T. Schlathölter, R. Hoekstra, and R. Morgenstern, J. Phys. B **31**, 1321 (1998).

[16] A. Reinköster, U. Werner, and H.O. Lutz, Europhys. Lett. **43**, 653 (1998).

[17] H. Tsuchida, A. Itoh, K. Miyabe, Y. Bitoh, and N. Imanishi, J. Phys. B **32**, 5289 (1999).

[18] A. Itoh, H. Tsuchida, T. Majima, and N. Imanishi, Phys. Rev. A **59**, 4428 (1999).

[19] A. Itoh, H. Tsuchida, T. Majima, S. Anada, A. Yogo, and N. Imanishi, Phys. Rev. A **61**, 12702 (1999).

[20] H. Hohmann, C. Callegari, S. Furrer, D. Grosenick, E.E.B. Campbell, and I.V. Hertel, Phys. Rev. Lett. **73**, 1919 (1994).

[21] H. Hohmann, R. Ehlich, S. Furrer, O. Kittelmann, J. Ringling, and E.E.B. Campbell, Z. Phys. D: At., Mol. Clusters **33**, 143 (1995).

[22] S. Hunsche, T. Starczewski, A. I'Huillier, A. Persson, C.-G. Wahlstöm, B. Van Linden van den Heuvell, and S. Svanberg, Phys. Rev. Lett. **77**, 1966 (1996).

[23] E.E.B. Campbell, T. Raz, and R.D. Levine, Chem. Phys. Lett. **253**, 261 (1996).

[24] N. Selberg, A. Bárány, C. Biedermann, C.J. Setterlind, H. Cederquist, A. Langereis, M.O. Larsson, A. Wännström, and P. Hvelplund, Phys. Rev. A **53**, 874 (1996).

[25] M.O. Larsson, P. Hvelplund, M.C. Larsen, H. Shen, H. Cederquist, and H.T. Schmidt, Int. J. Mass Spectrom. Ion Processes **177**, 51 (1998); Eur. Phys. J. D **5**, 283 (1999).

[26] J.M. Hansteen, O.M. Johnsen, and L. Kocbach, At. Data Nucl. Data Tables **15**, 305 (1975).

[27] P.L. Grande and G. Schiwietz, Phys. Rev. A **58**, 3796 (1998).

[28] G.M. de Azevedo, P.L. Grande, and G. Schiwietz, Nucl. Instrum. Methods Phys. Res. B **164/165**, 203 (2000).

[29] J. Opitz, H. Lebius, S. Tomita, B.A. Huber, P. Moretto Capelle, D. Bordenave Montesquieu, A. Bordenave Montesquieu, A.

Reinköster, U. Werner, H.O. Lutz, A. Niehaus, M. Benndorf, K. Haghighat, H.T. Schmidt, and H. Cederquist, Phys. Rev. A **62**, 22705 (2000).
[30] J.F. Ziegler, J.P. Biersack, and U. Littmark, *The Stopping and Range of Ions in Solids* (Pergamon, New York, 1999).
[31] W. Lotz, J. Opt. Soc. Am. **58**, 915 (1968).
[32] J.H. McGuire, Adv. At., Mol., Opt. Phys. **29**, 217 (1992).
[33] *CRC Handbook of Chemistry and Physics*, 67th ed.(CRC, Boca Raton, FL, 1987).
[34] J.P. Desclaux, At. Data Nucl. Data Tables **12**, 311 (1973).
[35] J.H. Miller and A.E.S. Green, Radiat. Res. **54**, 343 (1973).
[36] D. Tománek and M.A. Schluter, Phys. Rev. Lett. **67**, 2331 (1991).
[37] A. Itoh, H. Tsuchida, K. Miyabe, M. Imai, and N. Imanishi, Nucl. Instrum. Methods Phys. Res. B **129**, 363 (1997).
[38] R.E. Olson, J. Ullrich, and H. Schmidt-Böcking, Phys. Rev. A **39**, 5572 (1989).
[39] A. Bárány, in *Photonic, Electronic and Atomic Collisions, Proceedings of the XX International Conference on Photonic, Electronic and Atomic Collisions*, edited by F. Aumayr and H. Winter (World Scientific, Singapore, 1998), p. 641.
[40] S. Martin, L. Chen, A. Denis, and J. Désesquelles, Phys. Rev. A **59**, R1734 (1999).
[41] J. Jin, H. Khemliche, H. Prior, and Z. Xie, Phys. Rev. A **53**, 615 (1996).